Nuclear Inst. and Methods in Physics Research, A 1049 (2023) 168048

Contents lists available at ScienceDirect

Nuclear Inst. and Methods in Physics Research, A

journal homepage: www.elsevier.com/locate/nima

Full Length Article

Avalanche photodiode detection system enables X-ray communication up to 10 Mbps

Junqiu Yin [a], Yunpeng Liu [a,b,*], Feixu Xiong [a], Junxu Mu [a], Kai Miao [a], Xiaobin Tang [a,b]

[a] Department of Nuclear Science and Technology, Nanjing University of Aeronautics and Astronautics, Nanjing, 211106, China
[b] Key Laboratory of Nuclear Technology Application and Radiation Protection in Astronautics, Ministry of Industry and Information Technology, Nanjing 211106, China

ARTICLE INFO

Keywords:
Pulse X-ray signal detector
X-ray communication
Avalanche-photodiode
Fast amplifier
10 Mbps

ABSTRACT

As the core part of the X-ray communication (XCOM) system, the X-ray detector directly affects the data rate and bit error ratio (BER) performance. An avalanche photodiode (APD) with fast response time and high intern gain is chosen as the detector sensor to improve the data rate of XCOM. A three-stage fast preamplifier using radio frequency amplifier chips is designed to amplify the weak signal from the APD sensor. The bit synchronization signal acquisition and signal judgment modules are established to demodulate the detected pulse X-ray signals. The single photon pulse response and signal-to-noise ratio characteristic of the APD detector are tested. The pulse response width is only 25 ns. The BER characteristic with 211,709-bit pseudo-random sequence and the eye diagram of the XCOM system based on the developed APD detector are evaluated. Results show that the BER is zero at the data rate lower than 6 Mbps and reaches 1.98×10^{-4} at 10 Mbps under 55 kV anode voltage, 1.58 A filament current, and a 10 cm air channel. The designed APD detector increases the data rate of XCOM from the level of 1 Mbps to 10 Mbps, indicating its potential application for a higher data rate.

1. Introduction

X-ray communication (XCOM) is a wireless optical communication technology that uses X-ray beams as data transmission carriers [1]. Compared with the traditional signal carriers, X-ray beams have the characteristics of short wavelength and intense penetration. Therefore, XCOM has the advantages of a high theoretical communication rate (up to 40,000 Tbps) [2], small diffraction limit, and good directivity, which is considered the "next-generation aerospace communication technology" [3,4]. As shown in Fig. 1, the XCOM system is mainly composed of the modulator, the modulated X-ray source, the X-ray collimating/focusing optical system, the pulsed X-ray signal detector and the demodulator. The data transmission of the current XCOM system is realized by using the intensity modulation/direct detection technology due to the poor monochromaticity of the carrier X-ray. The main components determining the data rate of XCOM system include the pulsed X-ray sources and detectors.

At present, modulated X-ray sources mainly include light-controlled modulated X-ray tube (LMXT) [5], field emission X-ray tube (FEXT) [6], and grid-controlled modulated X-ray tube (GMXT) [7]. Benefiting from the development of high bandwidth power amplifiers, the latest GMXT optimized by our research group [7] can reach a 5 MHz repetition rate with high optical power. Through OOK modulation, this optimized GMXT may transmit data at a rate of 10 Mbps with a high signal-to-noise ratio (SNR). However, the current pulsed X-ray detectors only support about 1 Mbps communication rate due to their relatively low bandwidth.

The commonly used detectors in XCOM include microchannel plate (MCP) based detector [8,9], silicon drift detector (SDD) [10,11], and scintillator lutetium–yttrium oxyorthosilicate (LYSO) coupled with silicon photomultiplier (SiPM) detector [12]. The MCP detector is affected by the conversion efficiency of the photocathode, resulting in low sensitivity. The highest count rate of the fast SDD detector is only 10^6 cps [13], which is difficult to support the data rate above 2 Mbps. The charge-sensitive preamplifier assembled by the SDD discharges the charge at an unfixed period, which leads to random data loss. The LYSO-SiPM detector is mainly designed for the high-energy X-rays used in the "black barrier region" communication [14]. The however decay time of the coupled scintillator and the quenching time of the SiPM limit its bandwidth to several MHz, then hindering the further improvement of the data rate. The highest data rates reported for MCP, SDD and LYSO-SiPM detectors are 40 kbps with the bit error ratio (BER) of 6.49×10^{-2} [9], 100 kbps with the BER of 9.21×10^{-2} [15] and 1.12 Mbps with the BER of 1×10^{-5} [12], respectively. Therefore, a new high bandwidth and high sensitivity X-ray detector must be developed to improve the communication rate of the XCOM system.

* Corresponding author at: Department of Nuclear Science and Technology, Nanjing University of Aeronautics and Astronautics, Nanjing, 211106, China.
E-mail address: liuyp@nuaa.edu.cn (Y. Liu).

https://doi.org/10.1016/j.nima.2023.168048
Received 24 October 2022; Received in revised form 9 January 2023; Accepted 17 January 2023
Available online 18 January 2023
0168-9002/

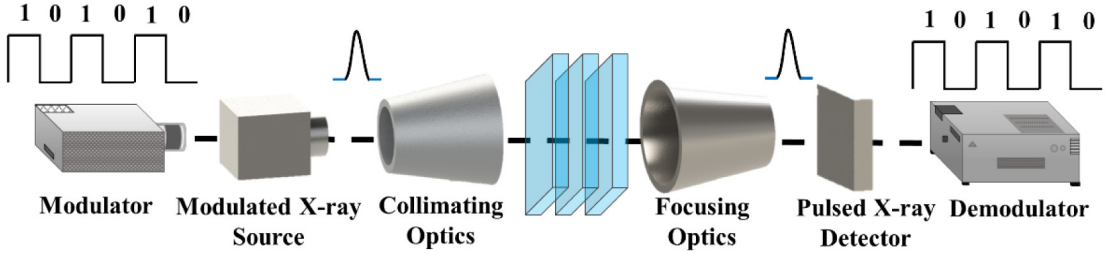

Fig. 1. Schematic of the general XCOM system.

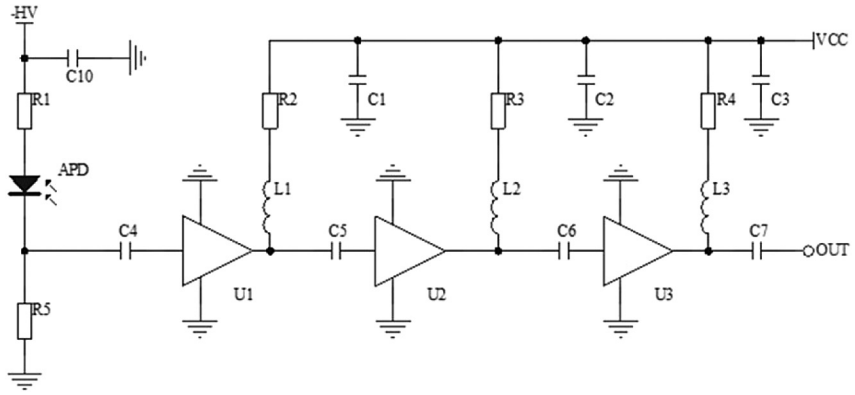

Fig. 2. Schematic diagram of the fast preamplifier.

The silicon avalanche photodiode (APD) detector is a semiconductor device that has internal signal amplification due to electron cascades [16]. The APD has a number of advantages, such as high counting rate, high sensitivity, and nanosecond or faster time response [17]. However, the actual bandwidth performance of the APD detector is not clear. Therefore, a single-photon test was conducted to know whether the APD detector can detect enough photons to demodulate the pulsed signal at high data rates or not. In this work, a high bandwidth detector based on APD sensor and fast preamplifier is proposed to meet the requirement of high data rate in XCOM. The bit synchronization signal acquisition and signal judgment modules are designed. The single photon response and SNR characteristic of the APD detector are tested. The BER characteristic at different data rates and eye diagram of the XCOM system based on the developed APD detector are evaluated.

2. Design of the APD detector system

2.1. APD sensor

The main parameters of the silicon APD sensor (C30703FH, Excelitas Technologies [18]) used in this work are listed in Table 1. This sensor has a reach-through structure and an intrinsic layer thickness of 120 μm, which has high detection efficiency for soft X-rays used in X-ray communications. This absorption thickness makes the sensor efficiency equal to 80% at 8.04 kev (Cu@Kα). The sensitive area of this sensor is 10 × 10 mm^2, which can receive sufficient X-ray photons for data transmission. This sensor typically is operated at high voltages of 400 V, where the gain is 50.

2.2. Fast preamplifier

Although the APD has internal gain, the voltage signal output by the sensor is still extremely weak. The MAR6-SM chip with the Darlington structure is selected for this work to adopt a three-stage cascade design for meeting the high gain requirement of the weak signal. The schematic diagram of the fast preamplifier is shown in Fig. 2. This commercial amplifier chip has a high bandwidth of 2 GHz and a high gain of 20 dB. The APD detector operates under direct current high-voltage bias provided by the preamplifier. For the bias circuit, coupling capacitors with large rated voltage are selected to prevent damage to the amplifier after high voltage breakdown. Given that the gain of one MAR6-SM chip is 20 dB, the preamplifier integrated with three stages has a gain of 60 dB. The fast preamplifier is designed and fabricated on a printed circuit board. The aluminum boxes and absorbers are applied to shield the environmental electromagnetic radiation. A fast preamplifier with high gain is implemented through the above measures. Fig. 3 shows the APD sensor with the fast preamplifier.

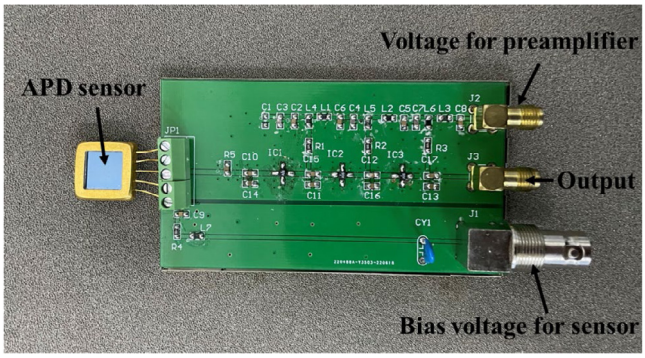

Fig. 3. Photograph of the APD sensor with the preamplifier.

Table 1
The Parameters of the used APD sensor.

Parameter	Value
Sensitive area	100 mm^2
Typical gain	50
Typical bias voltage	400 V
Typical dark current	250 nA
Capacitance	100 pF
Rise time	5 ns

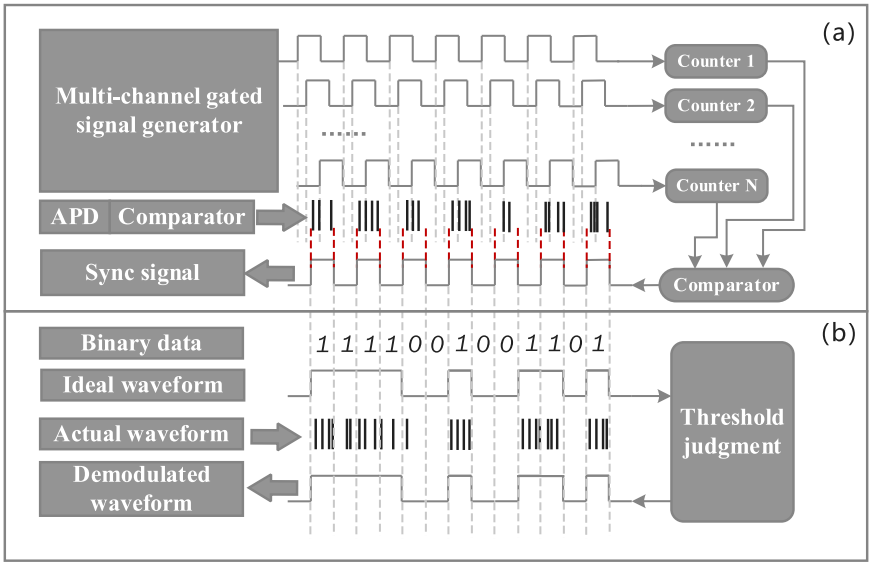

Fig. 4. Schematic of (a) signal synchronization bit acquisition and (b) signal judgment.

2.3. Signal demodulation method

The principle of obtaining the bit synchronization signal is shown in Fig. 4(a). The modulated X-ray source transmits the square wave signal with the same period and phase to acquire the signal synchronization bit before transmitting a valid signal. The comparator converts the analog pulse signal amplified by the preamplifier to form a photon sequence employing threshold discrimination. At the same time, the receiving end generates a multi-channel gating signal with the same cycle and different phases. The gating counter counts the photon sequences separately under the control of gating signals of different phases. The counting rule counts the input single photon pulses when the gating signal is high. The more the synchronized generated gating signal and the bit synchronization signal of the transmitting end, the larger the count value. The one with the largest count value is selected as the bit synchronization signal output by comparing the count value of the counter. With the described process, an accurate synchronization signal can be obtained by exploiting large gating and counter signals.

The principle diagram of signal discrimination is shown in Fig. 4(b). Signal judgment is based on the output data of the comparator. The photon counts in the high level "1" and the low level "0" are counted and averaged after the signal synchronization bit is acquired, thereby setting the threshold for signal discrimination. When the transmission signal is demodulated, the interval of each bit is divided in accordance with the bit synchronization signal, and the photon counts in the interval are counted. When the photon counts in the interval are greater than or equal to the threshold, the signal is judged to be a high level "1". Otherwise, the signal is judged to be a low level "0".

3. Performance test and results

An X-ray communication performance test system is built by using the developed APD detector and the laboratory's existing grid-controlled modulated X-ray tube (GMXT), as shown in Fig. 5. OOK modulation method is adopted in the experiment.

The X-ray signal transmission process is conducted as follows. GMXT generates an electron beam by heating the filament, and the electron beam bombards the anode target under the acceleration of the anode voltage to generate X-rays. The pseudorandom code is generated by the arbitrary waveform generator (AWG, RIGOLDG5102). The voltage signal output by AWG is amplified by the power amplifier (AIGTEK4315) and loaded on the grid of the X-ray tube. The electric field on the grid can control the on–off of the electron beam bombarding the anode target to realize the modulation of the signal. Signal generator modulation produces 0 and −5 V signals representing bit "1" and "0", respectively. The −5 V signal is amplified by the power amplifier to −65 V where the grid can completely cut off the electron beam. After passing through the air channel, the modulated X-ray signals reach the APD detector. The negative bias voltage of the detector is provided by a stable DC high-voltage power supply (ORTEC556). The detected signal is monitored by using a digital oscilloscope (RIGOLDMSO7024) with the sampling rate set to 500 MS/s. The captured signals are transmitted to a computer via the LabVIEW 2017 interface to be demodulated and evaluated offline. The APD detector and X-ray source are placed in a lead room. The distance between the detector and the X-ray source is 10 cm.

3.1. Single-photon pulse response

For a single-photon pulse signal, the steep rising edge can accurately determine the time slot of the signal that is needed to obtain the synchronization bit, and the fast falling time can reduce the interference of the previous pulse to the latter one. Therefore, the single-photon pulse response of the APD detector must be evaluated. Radioisotopes are ideal test sources due to their single-photon emission properties. In the experiment presented in this article, we use ^{238}Pu and ^{57}Co radioisotopes to conduct the single-photon test. The bias voltage is set to 400 V. In the response range of the APD detector, the photon energies with the highest emission probability of ^{238}Pu and ^{57}Co are 13.6 kev and 6.404 kev, respectively.

The test results are shown in Fig. 6. The width of single-photon pulse response of the APD is only 25 ns, whereas those of SDD and LYSO-SiPM detector are 2 μs [13] and 500 ns [19], respectively. Therefore, the response time and bandwidth of APD have obvious advantages over traditional XCOM detectors. The APD detector developed in this work is expected to achieve higher data rates.

3.2. Signal-to-noise ratio (SNR)

The SNR performance of the detectors is investigated under different anode voltages from 35 to 60 kV, filament currents from 1.42 to 1.62 A, and detector bias voltages from 250 to 450 V, as shown in Fig. 7. With the increase of anode voltage and filament current, the SNR of the detector is improved. The filament current and anode voltage affect the number and energy of electrons bombarding the anode target, respectively. The number of electrons is proportional to that of X-ray

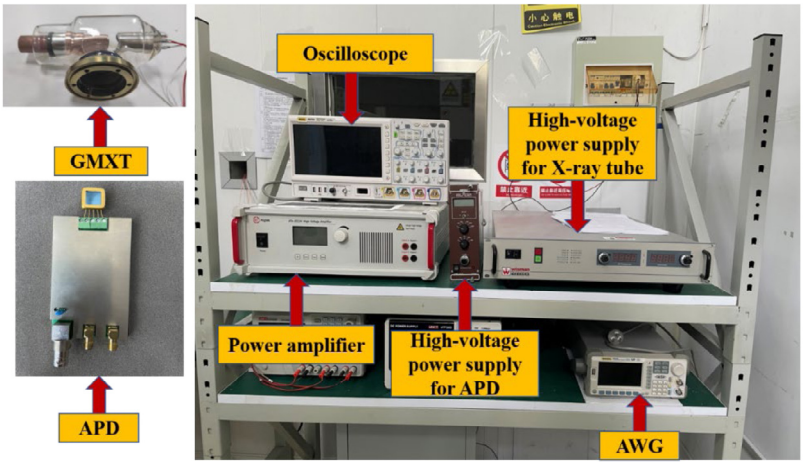

Fig. 5. Experimental setup of XCOM performance test system.

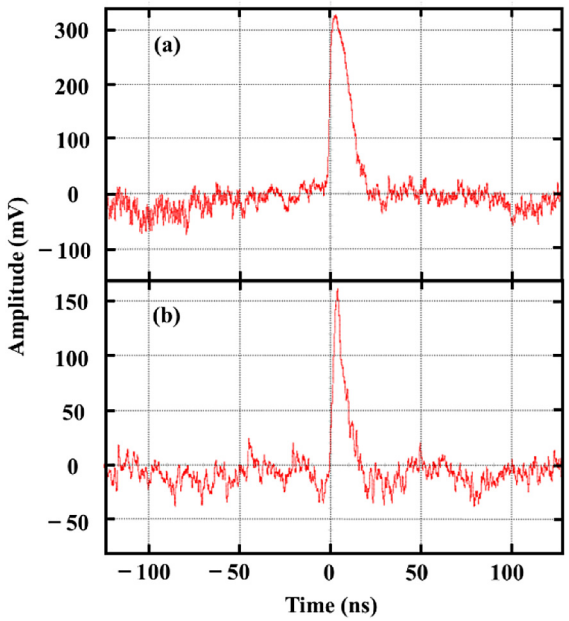

Fig. 6. Single photon test of (a) ^{238}Pu and (b) ^{57}Co.

photons, while the electron energy is proportional to the probability of bremsstrahlung that in turn affects the number and energy of X-ray photons.

Fig. 7(a) the 3D diagram shows of SNR under the effect of three parameters: filament current, anode voltage, and bias voltage. With the increase in detector bias, the area of high SNR (red area) keeps increasing, while the area of low SNR (purple area) shows anomalies at 450 V. The internal gain and the consequent signal amplitude of the detector increase with the bias voltage. While the dark current of the detector will also escalate, resulting in the augmented levels of noise power. When the bias voltage rises to 450 V, the gain and signal amplitude almost reach saturation, and the dark current is still growing, thus causing a little decline in SNR.

Figs. 7(b), (c), and (d) show the effect of SNR by anode voltage, filament current, and bias voltage, respectively. The variation of SNR in Fig. 7(d) is much smaller than that of the other two figures. This finding indicates that changing the detector bias has less effect on the SNR than changing the parameters of the X-ray source. Therefore, increasing the number of photons is more important than increasing the magnitude of a single photon. For the demodulation method based on the photon counting strategy, high-amplitude X-ray photons are easier to identify, but the number of X-ray photons is the key to signal judgment.

3.3. Bit error ratio (BER)

The anode voltage, filament current and bias voltage are set to 55 kV, 1.58 A and 400 V for the BER test, respectively. The pseudo random binary sequence PRBS7 is adopted. A total of 211,709 bits are sampled for offline demodulation at 1–10 Mbps. The results are presented in Fig. 8.

The signal can be demodulated without error when the data rate does not exceed 6 Mbps after the transmission test of 211,709-bit pseudorandom sequence. With the further improvement of the communication rate, the BER increases gradually. At the data rate of 10 Mbps, the BER is 1.98×10^{-4}. The waveforms of APD and power amplifier of 1 and 10 Mbps are shown in Fig. 9. As can be seen the increase in the data rate, the power amplifier waveform is gradually distorted. This condition suppresses the electron emission at a high level and releases some electrons at a low level, resulting in error bits. Moreover, as the data rate increases, the number of photons in a unit bit decreases, thereby increasing the probability of misjudgment for high-level signals.

By counting the bit errors, it can be found that 83.3% of the detected errors are associated with the 1-as-0 interpretation error. This condition is because insufficient photons are observed in some time slots due to the jitter of the X-ray tube [20]. With the increase in the communication rate, the effect of jitter becomes more pronounced. Therefore, the main cause of bit errors at high communication rates is that the X-ray tube emits insufficient X-ray photons per bit.

3.4. Eye diagram

The single-photon response test shows that the APD detector has good bandwidth performance, and the main factor affecting the communication performance is the number of photons per bit. Therefore, we use the eye diagram to evaluate the stability of the number of photons. The eye diagrams are drawn after averaging the amplitude of the signal within each bit at 1 Mbps and 10 Mbps, as shown in Fig. 10. The average of the amplitude can reflect the number of photons to some extent. In this way, the crossing points in the eye diagram can only reflect the stability of the amplitude, regardless of the rise and fall time of the signal. Some main features of the eye diagram are extracted for qualitative analysis.

Under the condition of 1 and 10 Mbps data rates, the image below the crossing point is very clear. This condition indicates that high levels have very little crosstalk for low levels, which is the contribution of

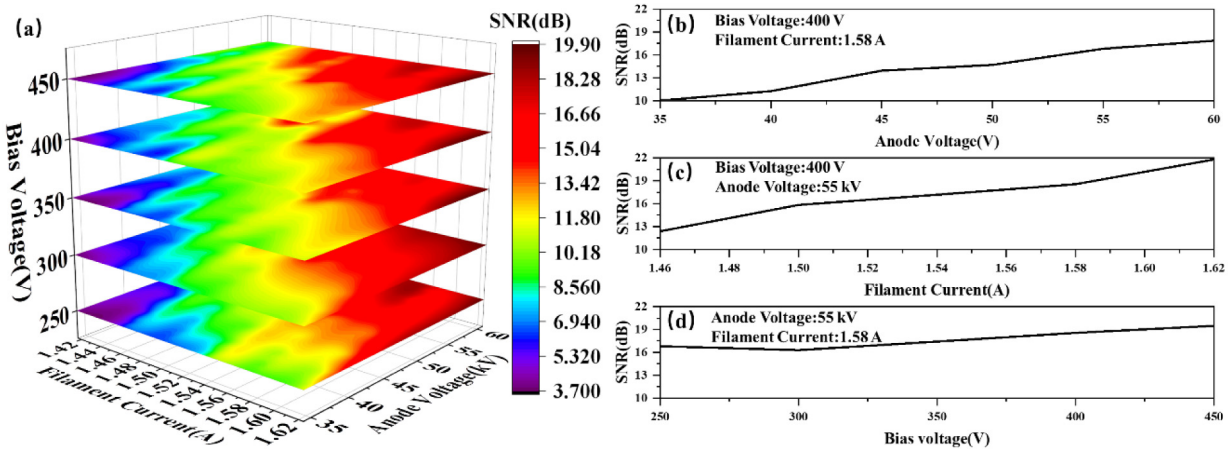

Fig. 7. (a) SNR vs. anode voltage, filament current and bias voltage; (b) SNR vs. anode voltage; (c) SNR vs. filament current; (d) SNR vs. bias voltage.

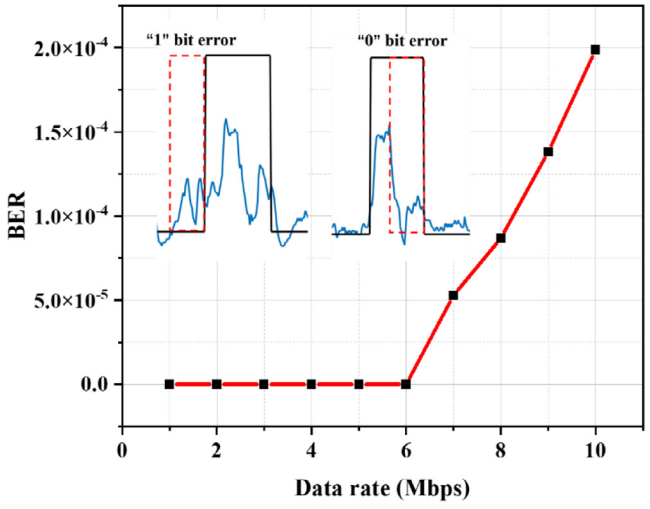

Fig. 8. BER vs. different date rates.

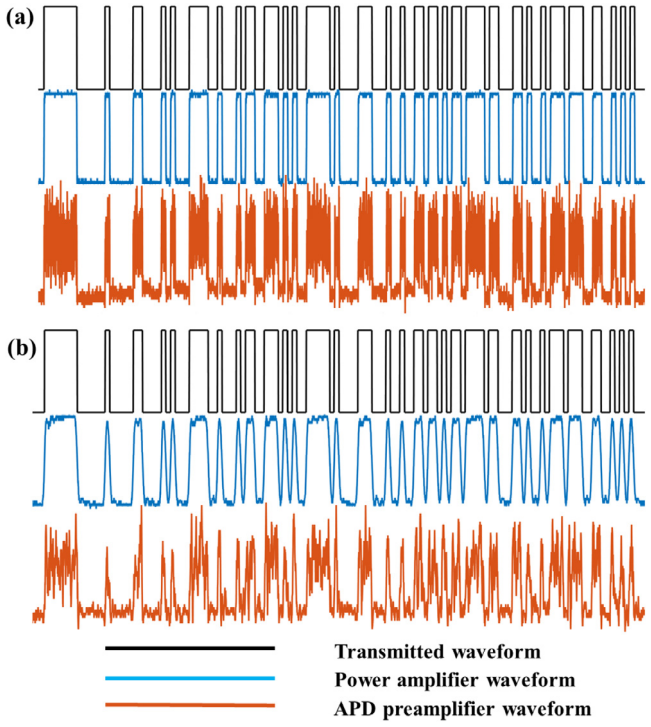

Fig. 9. Waveforms of APD and power amplifier at (a) 1 Mbps and (b) 10 Mbps.

the fast rise time of the APD sensor and the high bandwidth of the preamplifier. When the data rate reaches 10 Mbps, crosstalk starts to become apparent at high levels. As the data rate increases, the number of photons in a unit bit decreases, resulting in serious fluctuations in the high level. This phenomenon corresponds exactly to the higher probability of misjudging "1" as "0" than that of "0" as "1" at 10 Mbps.

The high-level eyeliner of 1 Mbps is thinner than that of 10 Mbps by comparing the upper limits of the two eye diagrams, which indicating that there are large distortions at 10 Mbps. The detector output signal appears as discrete photon pulses due to the strong particle nature of X-rays. The monochromaticity of the X-ray source is poor, and the energy of the X-ray has a certain spectral distribution. The APD energy resolution performance is not optimized specifically, so some fluctuations are observed. The width of per bit is shorter at 10 Mbps, so the number of photons and the amplitude of the signal show greater variation. However, the low-level eyeline of 1 Mbps is thicker than that of 10 Mbps by comparing the lower limits of the two eye diagrams. This condition is because periodic fluctuations occur in the detector's baseline, and this phenomenon appears to be more pronounced on the 1 Mbps timescale.

The two eye diagrams have an area with a large crossing point, indicating that the average amplitude of per bit have large fluctuations. The generation of X-ray photons exhibits uncertainty due to the emission mechanism of bremsstrahlung. The crossing point ratio for 1 Mbps is about 50%, while that for 10 Mbps is less than 50%. Therefore, the bit width of high level is smaller than that of low level at 10 Mbps. The reason is that the power amplifier distorts at high frequencies, suppressing the number of electrons bombarding the anode target at the rising and falling moments of the high level.

4. Conclusion

An X-ray detector using fast response time and high internal gain APD sensor is designed for high data rate XCOM. A fast preamplifier is designed with three cascaded amplification stages to detect a signal photon. On the basis of the photon counting strategy, the demodulation method of the signal output by the APD preamplifier is established. The width of the single-photon pulse signal output by the preamplifier is about 25 ns, which indicates that the APD detector is expected to achieve higher data rate. Under the condition of 55 kV anode voltage, 1.58 A filament current, and 10 cm air channel, the APD detector is tested with 211,709-bit pseudo-random sequence. The BER is zero

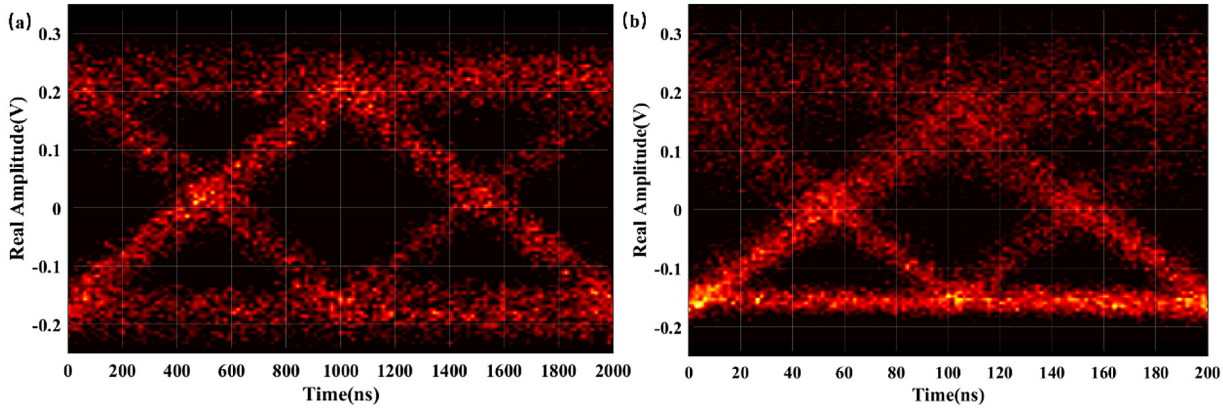

Fig. 10. Eye diagram at (a) 1 Mbps and (b) 10 Mbps.

at data rate lower than 6 Mbps and is 1.98×10^{-4} at 10 Mbps. By analyzing the eye diagram and waveform from the detector, bit errors are mainly caused by the distortion of the power amplifier signal at high frequencies and the jitter of the X-ray tube. These results show that the developed APD detector system can meet the communication requirements of 10 Mbps. The developed APD detector has potential to support higher communication rate in XCOM, if the pulse emission characteristic of the modulated X-ray source is improved in the future. This work processes the development of XCOM, a revolutionary technology, for engineering applications in the field of deep space communication.

Declaration of competing interest

The authors declare that they have no known competing financial interests or personal relationships that could have appeared to influence the work reported in this paper.

Data availability

Data will be made available on request.

Acknowledgments

This work was supported by the Foundation of Graduate Innovation Center in NUAA, China (Grant No. xcxjh20210617).

References

[1] B. Zhao, et al., Next generation of space wireless communication technology based on X-ray, Acta Photonica Sin. 42 (7) (2013).
[2] George Porter, See straight through data center bandwidth limitations with X-rays, 2013.
[3] Peter J. Winzer, Would scaling to extreme ultraviolet or soft X-ray communications resolve the capacity crunch? J. Lightwave Technol. 36 (24) (2018) 5786–5793.
[4] Keith Gendreau, Next-generation communications: demonstrating the world's first X-ray communication system, NASA, Rep. no. FS-2007-10-103-GSFC (TT# 7), 2007.
[5] Hao Xuan, et al., Light-controlled pulsed x-ray tube with photocathode, Chin. Phys. B 30 (11) (2021) 118502.
[6] Sheng Lai, et al., X-ray high frequency pulse emission characteristic and application of CNT cold cathode x-ray source cathode x-ray source, Nanotechnology 33 (7) (2021) 075201.
[7] Zhaopeng Feng, et al., Optimization and testing of groove-shaped grid-controlled modulated X-ray tube for X-ray communication, Nucl. Instrum. Methods Phys. Res. A 1026 (2022) 166218.
[8] Qingyong Zhou, et al., The test and analysis on pulse signal detection abilities of the X-ray detector MCP for pulsar navigation, in: China Satellite Navigation Conference, Springer, Singapore, 2017.
[9] Li Yao, et al., Bit error rate analysis of the spatial X-ray communication system, Infrared Laser Eng. 47 (6) (2018) 622001-0622001.
[10] Gregory Prigozhin, et al., NICER instrument detector subsystem: description and performance, in: Space Telescopes and Instrumentation 2016: Ultraviolet To Gamma Ray, Vol. 9905, SPIE, 2016.
[11] Yong-an Liu, et al., X-ray communication experiment using photocathode x-ray tube, in: Seventh Symposium on Novel Photoelectronic Detection Technology and Applications, Vol. 11763, SPIE, 2021.
[12] Junxu Mu, et al., Design and performance test of pulse X-ray receiver based on LYSO-SiPM for X-ray communication, J. Lightwave Technol. (2022).
[13] Neng Xu, et al., Silicon drift detector applied to X-ray pulsar navigation, Nucl. Instrum. Methods Phys. Res. A 927 (2019) 429–434.
[14] Huan Li, et al., Potential application of X-ray communication through a plasma sheath encountered during spacecraft reentry into earth's atmosphere, J. Appl. Phys. 121 (12) (2017) 123101.
[15] Li Yao, Research on the key technologies of space X-ray communication, in: Xi'an Institute of Optics & Precision Mechanics, (Ph.D. dissertation), Chinese Academy of Sciences, Xi'an, China, 2019.
[16] Y. Yatsu, et al., Study of avalanche photodiodes for soft X-ray detection below 20 keV, Nucl. Instrum. Methods Phys. Res. A 564 (1) (2006) 134–143.
[17] Alfred Q.R. Baron, et al., Silicon avalanche photodiodes for direct detection of X-rays, J. Synchrotron Radiat. 13 (2) (2006) 131–142.
[18] Zhenjie Li, et al., Development of an integrated four-channel fast avalanche-photodiode detector system with nanosecond time resolution, Nucl. Instrum. Methods Phys. Res. A 870 (2017) 43–49.
[19] Yunpeng Liu, et al., Performance analysis of LYSO–SiPM detection module for X-ray communication during spacecraft reentry blackout, Nucl. Instrum. Methods Phys. Res. A 1013 (2021) 165673.
[20] Wenxuan Chen, et al., Experimental evaluation of an OFDM-PWM-based X-ray communication system, Opt. Express 29 (3) (2021) 3596–3608.